AIAA JOURNAL
Vol. 38, No. 2, February 2000

Single- vs Multilayer Plate Modelings on the Basis of Reissner's Mixed Theorem

Erasmo Carrera*
Politecnico di Torino, 10129 Turin, Italy

The use of Reissner's mixed variational theorem (Reissner, E., "On a Certain Mixed Variational Theory and a Proposed Applications," *International Journal for Numerical Methods in Engineering*, Vol. 20, 1984, pp. 1366–1368; Reissner, E., "On a Mixed Variational Theorem and on a Shear Deformable Plate Theory," *International Journal of Numerical Methods in Engineering*, Vol. 23, 1986, pp. 193–198) to analyze laminated plate structures is examined. The two cases of single-layer and multilayer models have been compared. Governing equilibrium and constitutive equations have been derived in a unified manner. Navier-type closed-form solutions are presented for the particular case of cross-ply simply supported plates. Thin and thick, as well as symmetrically and asymmetrically laminated plates, have been investigated. Displacements and transverse stresses have been evaluated and compared with available mixed two-dimensional results and three-dimensional solutions. The following have been concluded: 1) Reissner's mixed theorem is a very suitable tool to analyze laminated structures. 2) Multilayer modelings lead to an excellent agreement with exact solution for both displacement and transverse stress evaluations. Such an agreement, which has been confirmed for very thick geometries ($a/h \leq 4$), does not depend on laminate layouts. No remarkable differences have been found for stresses evaluated a priori by the assumed model with respect to exact results. 3) Single-layer analyses lead to an accurate description of the response of thick plates. Major discrepancies have been found for very thick plate geometries with exact solutions. Nevertheless, their accuracy is very much subordinate to the order of the used expansion as well as to laminated layouts. Better transverse stress evaluations are obtained upon integration of three-dimensional equilibrium equations a posteriori than those furnished a priori. This trend has been confirmed for both thick and thin plates.

I. Introduction

STARTING from the early works by Murakami[1] and Toledano and Murakami,[2–4] the use of Reissner's mixed variational theorem (RMVT)[5,6] has played an increasing role in the field of accurate modeling of multilayered plates[7–10] and shell structures.[11–15] As the main task, RMVT permits one to assume two independent, piecewise continuous fields for displacements and for transverse shear and normal stresses. As amply discussed by the author,[7] RMVT can be applied in both single-layer models [or equivalent single-layer models (ESLM)] and multilayers [or layerwise models (LWM)]. ESLM preserve the independence of the number of the independent variables from the numbers of the N_l layers, whereas the number of the unknown variables remains N_l dependent in the LWM. From a computational point of view, LWM result in being more expensive than ESLM. Normally, ESLM applications are in fact preferred to solve practical problems involving composite materials where the number of constitutive layers can be very high. ESLM are also preferred in problems that involve nonlinear calculation, for instance postbuckling analysis of plate and shell structures. Single-layer models lead to a set of constitutive equations, the number of which is N_l dependent (see Sec. V). From this point of view, to call them single layer does not seem very appropriate. Their use can, however, be justified by the fact that the stress variables can be eliminated in the numerical solution process.

Examples of RMVT application to laminated plates in the framework of the single-layer model were presented in Refs. 1 and 3. Through-the-thickness linear in-plane displacement field was assumed in Ref. 1. A zigzag function (see Sec. III.A) was introduced to reproduce the discontinuity of the first derivative in correspondence to each layer interface. Transverse normal stresses were neglected, and transverse shear fields were assumed to be parabolic in each layer. The obtained results that were related to cylindrical bending of cross-ply, symmetrically laminated plates showed improved description of the in-plane response with respect to first-order shear deformation theory. Extension to cubic displacement expansion was subsequently considered by Toledano and Murakami.[3] Fourth-order transverse normal and shear-stress fields were then implemented. Better results than those in Ref. 1 were obtained, and applications to asymmetrically laminated plates were presented. Transverse shear-stress results were not quoted in Ref. 3. Shell applications of the theory in Ref. 1 were developed by Bhaskar and Varadan[11] and Jing and Tzeng.[12] Bhaskar and Varadan[11] underlined the great limitation of transverse shear stress a priori evaluated by the assumed model. Finite element applications of the mentioned model have also been developed. Linear analysis of thick plates was discussed by Rao and Meyer-Piening.[16] Linear and geometrically nonlinear static and dynamic analyses were considered by Carrera and coauthors.[17–21] Partial implementation to shell elements was proposed by Bhaskar and Varadan[22] and Carrera and Parisch.[23]

The limitations of single-layer analyses were known to Toledano and Murakami,[2] who applied RMVT in the field of a multilayers models. A linear in-plane displacement expansion was expressed in terms of the interface values in each layer, whereas transverse shear stresses were assumed to be parabolic. The accuracy of the resulting theories was layout independent. Transverse normal stress and the related effects were discarded, and the analysis showed severe limitations in the analysis of thick plates. A more comprehensive evaluation of multilayer theories for the case of linear and parabolic expansions was considered by the author in Ref. 9, where applications to the static analysis of plates were presented. Subsequent works extended the analysis to the dynamics case[10] and shell geometry.[13–15] In Ref. 9 the author showed that RMVT leads to a quasi-three-dimensional description of the in-plane and out-of plane response. In particular, transverse stresses were determined a priori with excellent accuracy.

From the preceding literature overview, the relevance of RMVT as a tool to analyze multilayered structures appears evident. For the sake of brevity, a comparison to other available approaches to laminated structures is not included in the present paper. Those readers who are interested can refer to the just-mentioned papers and to the recent book by Reddy.[24] In comparison to the very interesting and recent works by Cho and Parmerter[25] and Lee et al.,[26] the

Received 15 July 1998; revision received 20 April 1999; accepted for publication 22 June 1999.

*Research Professor, Dipartimento di Ingegneria Aeronautica e Spaziale.

mixed ESL theories herein proposed describe interlaminar continuous transverse normal stresses σ_{zz}.

In spite of the remarkable number of previously mentioned research works, there is no available analysis in which an extensive comparison of multilayer vs single-layer modelings, formulated on the basis of Reissner's theorem, is presented. The author is convinced that such a comparison is of prime interest for the structural analyst of multilayered structures. For instance, the number of the constitutive layers can be very high (10, 20, 30) in composite applications; as a consequence, the number of the independent variables can be very different for ESLM than for layerwise (LW) implementations. From this point of view, the knowledge of the accuracy of different theories could offer the analyst the possibility of weighing the costs of using a certain number of unknown variables to be used in the calculation with respect to the related accuracy. This is a fundamental information in practical problems. Such information becomes essential for computational application as well as nonlinear analysis when the computation cost becomes prohibitive. The aim of the present work is directed toward removing this absence.

In this paper the use of RMVT is established in a form that is suitable for both multilayer and single-layer analysis. Displacement and transverse stress fields, as well as governing equations, have been written in a unified manner. To make a comprehensive numerical comparison, several new single-layer and multilayer theories have been implemented. Attention has here been restricted to plate geometry.

II. Preliminary

The geometry and coordinate system of the laminated plates of N_l layers are shown in Fig. 1. The integer k, which is extensively used as both subscript and superscript, denotes the layer number that starts from the plate bottom. x and y are the plate middle surface Ω^k coordinates. Γ^k is the layer boundary on Ω^k. z and z_k are the plate and layer thickness coordinates; h and h_k denote plate and layer thickness, respectively. $\zeta_k = 2z_k / h_k$ is the nondimensioned local plate-coordinate; A_k will denote the k-layer thickness domain. Symbols not affected by k subscript/superscripts refer to the whole plate.

The lamina are supposed to be homogeneous and to operate in the linear elastic range. Stiffness coefficients are employed in standard form of the Hooke's law for the anisotropic k lamina. It reads $\sigma_i = \tilde{C}_{ij}\epsilon_j$ where sub-indices i and j, ranging from 1 to 6, stand for the index couples 11, 22, 33, 13, 23, and 12, respectively. The material is assumed to be orthotropic as specified by $\tilde{C}_{14} = \tilde{C}_{24} = \tilde{C}_{34} = \tilde{C}_{64} = \tilde{C}_{15} = \tilde{C}_{25} = \tilde{C}_{35} = \tilde{C}_{65} = 0$. This implies that σ^k_{xz} and σ^k_{yz} depend only on ϵ^k_{xz} and ϵ^k_{yz}. In matrix form

$$\sigma^k_{\mathrm{pH}} = \tilde{\boldsymbol{C}}^k_{\mathrm{pp}}\epsilon^k_{\mathrm{pG}} + \tilde{\boldsymbol{C}}^k_{\mathrm{pn}}\epsilon^k_{\mathrm{nG}}, \qquad \sigma^k_{\mathrm{nH}} = \tilde{\boldsymbol{C}}^k_{\mathrm{np}}\epsilon^k_{\mathrm{pG}} + \tilde{\boldsymbol{C}}^k_{\mathrm{nn}}\epsilon^k_{\mathrm{nG}} \tag{1}$$

where

$$\tilde{\boldsymbol{C}}^k_{\mathrm{pp}} = \begin{bmatrix} \tilde{C}^k_{11} & \tilde{C}^k_{12} & \tilde{C}^k_{16} \\ \tilde{C}^k_{12} & \tilde{C}^k_{22} & \tilde{C}^k_{26} \\ \tilde{C}^k_{16} & \tilde{C}^k_{26} & \tilde{C}^k_{66} \end{bmatrix}, \qquad \tilde{\boldsymbol{C}}^k_{\mathrm{pn}} = \tilde{\boldsymbol{C}}^{k^T}_{\mathrm{np}} = \begin{bmatrix} 0 & 0 & \tilde{C}^k_{13} \\ 0 & 0 & \tilde{C}^k_{23} \\ 0 & 0 & \tilde{C}^k_{36} \end{bmatrix}$$

$$\tilde{\boldsymbol{C}}^k_{\mathrm{nn}} = \begin{bmatrix} \tilde{C}^k_{44} & \tilde{C}^k_{45} & 0 \\ \tilde{C}^k_{45} & \tilde{C}^k_{55} & 0 \\ 0 & 0 & \tilde{C}^k_{66} \end{bmatrix}$$

Bold letters denote arrays. The superscript T signifies array transposition. The subscripts n and p denote transverse (out-of-plane, normal) and in-plane values, respectively. Therefore,

$$\sigma^k_p = \{\sigma^k_{xx}, \sigma^k_{yy}, \sigma^k_{xy}\}, \qquad \sigma^k_n = \{\sigma^k_{xz}, \sigma^k_{yz}, \sigma^k_{zz}\}$$

$$\epsilon^k_p = \{\epsilon^k_{xx}, \epsilon^k_{yy}, \epsilon^k_{xy}\}, \qquad \epsilon^k_n = \{\epsilon^k_{xz}, \epsilon^k_{yz}, \epsilon^k_{zz}\}$$

Subscript H denotes stresses evaluated by Hooke's law, and subscript G denotes strain from the geometrical relation equation (3). Equation (1) is used in conjunction with a standard displacement formulation, whereas, for the adopted mixed solution procedure, the stress-strain relationships are conveniently put in the following mixed form:

$$\sigma^k_{\mathrm{pH}} = \boldsymbol{C}^k_{\mathrm{pp}}\epsilon^k_{\mathrm{pG}} + \boldsymbol{C}^k_{\mathrm{pn}}\sigma^k_{\mathrm{nM}}, \qquad \epsilon^k_{\mathrm{nH}} = \boldsymbol{C}^k_{\mathrm{np}}\epsilon^k_{\mathrm{pG}} + \boldsymbol{C}^k_{\mathrm{nn}}\sigma^k_{\mathrm{nM}} \tag{2}$$

where both stiffness and compliance coefficients are employed. The subscript M states that the transverse stresses are those of the assumed model in Eq. (12) (see the next sections). The relation between the arrays of coefficients in the two forms of Hooke's law is simply found:

$$\boldsymbol{C}^k_{\mathrm{pp}} = \tilde{\boldsymbol{C}}^k_{\mathrm{pp}} - \tilde{\boldsymbol{C}}^k_{\mathrm{pn}}\tilde{\boldsymbol{C}}^{k^{-1}}_{\mathrm{nn}}\tilde{\boldsymbol{C}}^k_{\mathrm{np}}, \qquad \boldsymbol{C}^k_{\mathrm{pn}} = \tilde{\boldsymbol{C}}^k_{\mathrm{pn}}\tilde{\boldsymbol{C}}^{k^{-1}}_{\mathrm{nn}}$$

$$\boldsymbol{C}^k_{\mathrm{np}} = -\tilde{\boldsymbol{C}}^{k^{-1}}_{\mathrm{nn}}\tilde{\boldsymbol{C}}^k_{\mathrm{np}}, \qquad \boldsymbol{C}^k_{\mathrm{nn}} = \tilde{\boldsymbol{C}}^{k^{-1}}_{\mathrm{nn}}$$

Superscript -1 denotes an inversion of the array.

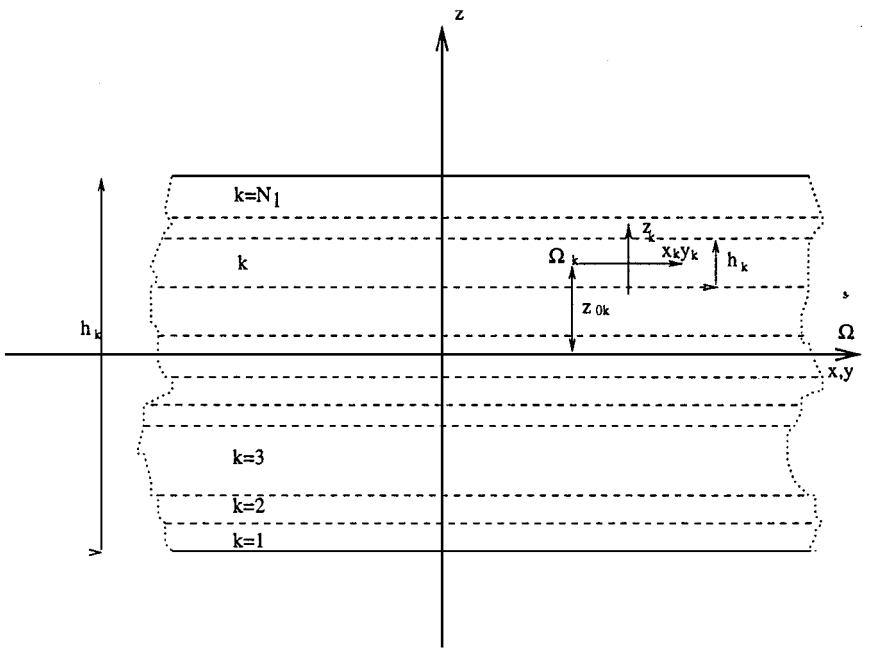

Fig. 1 Multilayered plate.

The strain components ϵ_p^k, ϵ_n^k are linearly related to the displacements $\boldsymbol{u}^k$ ($\{u_x^k, u_y^k, u_z^k\}$), according to the following geometrical relations:

$$\epsilon_{pG}^k = \boldsymbol{D}_p \boldsymbol{u}^k, \qquad \epsilon_{nG}^k = \boldsymbol{D}_n \boldsymbol{u}^k \tag{3}$$

$\boldsymbol{D}_p$ and $\boldsymbol{D}_n$ denotes in-plane and out-of-plane differential operators:

$$\boldsymbol{D}_p = \begin{bmatrix} \partial_x & 0 & 0 \\ 0 & \partial_y & 0 \\ \partial_y & \partial_x & 0 \end{bmatrix}, \qquad \boldsymbol{D}_n = \begin{bmatrix} \partial_z & 0 & \partial_x \\ 0 & \partial_z & \partial_y \\ 0 & 0 & \partial_z \end{bmatrix}$$

III. Single-Layer Theories or ESLM

The Reissner's mixed variational theorem permits one to assume two independent fields for the displacement and transverse stress fields.

A. Displacement Field

By referring to the Murakami idea,[1] the zigzag form of the displacements fields can be reproduced in an equivalent single-layer description. Such an idea consists of adding a zigzag term into a classical Taylor-type expansion in the thickness plate direction of the unknown displacements in the neighborhood of the reference plate surface Ω (Fig. 2a). The displacement model in Refs. 1 and 3 is herein written in the following generalized form:

$$\boldsymbol{u} = \boldsymbol{u}_0 + (-1)^k \zeta_k \boldsymbol{u}_Z + z^r \boldsymbol{u}_r, \qquad r = 1, 2, \ldots, N \tag{4}$$

N is a free parameter of the model. The repeated indices r are summed over their ranges. Subscript 0 denotes values related to the plate reference surface Ω, whereas subscript z refers to the introduced zigzag term. Higher-order distributions in the z direction are introduced by the r polynomials. To give a unified form for the assumed models, the same notations that will be employed in the layerwise description should be conveniently used in Eqs. (4), which are therefore rewritten as

$$\boldsymbol{u} = F_t \boldsymbol{u}_t + F_b \boldsymbol{u}_b + F_r \boldsymbol{u}_r = F_\tau \boldsymbol{u}_\tau$$
$$\tau = t, b, r, \qquad r = 1, 2, \ldots, N \tag{5}$$

Subscript b denotes values related to the plate reference surface Ω ($\boldsymbol{u}_b = \boldsymbol{u}_0$), whereas subscript t refers to the introduced zigzag term ($\boldsymbol{u}_t = \boldsymbol{u}_Z$). The functions F_τ assume the following explicit form:

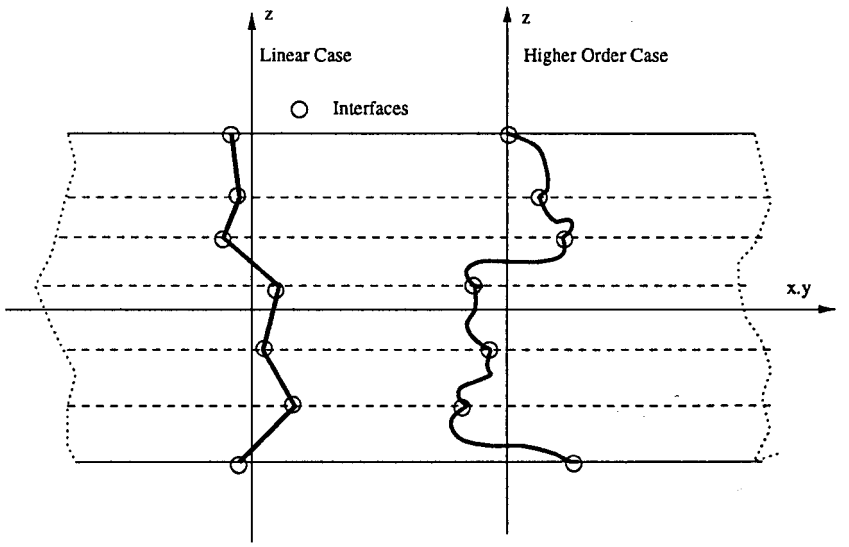

a) Multilayer

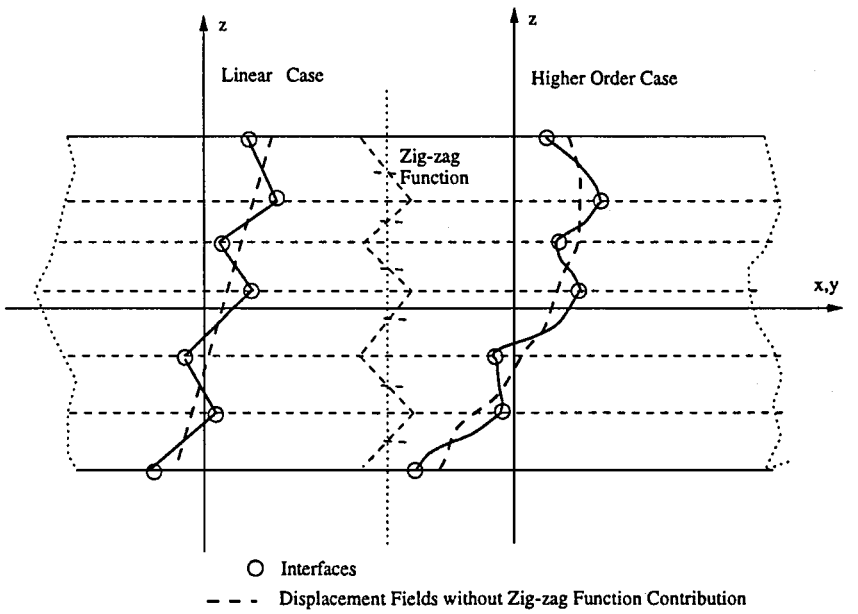

b) Single layer

Fig. 2 Fields assumed in the thickness plate directions.

$$F_b = 1, \qquad F_t = (-1)^k \zeta_k, \qquad F_r = z^r \qquad r = 1, 2, \ldots, N \tag{6}$$

To notice that F_t assumes the values ± 1 in correspondence to the bottom and the top interface of the k layer (Fig. 2a), $\boldsymbol{u}_t$ is taken constant in Eqs. (5). This fact consists of the fundamental limitation of the considered single-layer models.

B. Transverse Stress Field

The thickness expansion used for displacement variables in Eqs. (5) is not suitable for transverse stresses: for instance, homogeneous top-bottom plate surface conditions could not be imposed. Therefore, transverse stresses are herein described by means of a layerwise description[1,3,7,9]:

$$\sigma^k_{\mathrm{nM}} = F_t \sigma^k_{\mathrm{nt}} + F_b \sigma^k_{\mathrm{nb}} + F_r \sigma^k_{\mathrm{nr}} = F_\tau \sigma^k_{\mathrm{n}\tau}$$

$$\tau = t, b, r, \qquad r = 2, 3, \ldots, N, \qquad k = 1, 2, \ldots, N_l \tag{7}$$

In contrast to Eqs. (5), subscripts t and b denote values related to the layer top and bottom surface, respectively. They consist of the linear part of the expansion. The thickness functions $F_\tau(\zeta_k)$ have been defined by

$$F_t = (P_0 + P_1)/2, \qquad F_b = (P_0 - P_1)/2, \qquad F_r = P_r - P_{r-2} \qquad r = 2, 3, \ldots, N \tag{8}$$

in which $P_j = P_j(\zeta_k)$ is the Legendre polynomial of the j order defined in the ζ_k domain: $-1 \le \zeta_k \le 1$. A fourth-order case will be used in the numerical investigations; related polynomials are

$$P_0 = 1, \qquad P_1 = \zeta_k, \qquad P_2 = (3\zeta_k^2 - 1)/2$$

$$P_3 = (5\zeta_k^3/2) - (3\zeta_k/2), \qquad P_4 = (35\zeta_k^4/8) - (15\zeta_k^2/4) + \tfrac{3}{8}$$

The chosen functions have the following properties:

$$\zeta_k = \begin{cases} 1: & F_t = 1, \quad F_b = 0, \quad F_r = 0 \\ -1: & F_t = 0, \quad F_b = 1, \quad F_r = 0 \end{cases} \tag{9}$$

The top and bottom values have been used as unknown variables. The interlaminar transverse shear and normal stress continuity can therefore be easily linked:

$$\sigma^k_{\mathrm{nt}} = \sigma^{(k+1)}_{\mathrm{nb}}, \qquad k = 1, N_l - 1 \tag{10}$$

In those cases in which top/bottom-shell stress values are prescribed (zero or imposed values), the following additional equilibrium conditions must be accounted for:

$$\sigma^1_{\mathrm{nb}} = \bar{\sigma}_{\mathrm{nb}}, \qquad \sigma^{N_l}_{\mathrm{nt}} = \bar{\sigma}_{\mathrm{nt}} \tag{11}$$

where the overbar is the imposed value in correspondence to the plate boundary surfaces. Examples of linear and higher-order fields have been plotted in Fig. 2b.

IV. Multilayer Theories or LWM

Multilayer modelings were mainly proposed to remove the independence of the zigzag amplitude $\boldsymbol{u}_Z$ by the layer. Layerwise fields are assumed for both displacement and stress variables as in Eqs. (7):

$$\boldsymbol{u}^k = F_t \boldsymbol{u}^k_t + F_b \boldsymbol{u}^k_b + F_r \boldsymbol{u}^k_r = F_\tau \boldsymbol{u}^k_\tau, \qquad \tau = t, b, r \qquad r = 2, 3, \ldots, N$$

$$\sigma^k_{\mathrm{nM}} = F_t \sigma^k_{\mathrm{nt}} + F_b \sigma^k_{\mathrm{nb}} + F_r \sigma^k_{\mathrm{nr}} = F_\tau \sigma^k_{n\tau}, \qquad k = 1, 2, \ldots, N_l \tag{12}$$

In addition to Eqs. (10), the compatibility of the displacement reads

$$\boldsymbol{u}^k_t = \boldsymbol{u}^{(k+1)}_b, \qquad k = 1, N_l - 1 \tag{13}$$

Equations (12) refer to the same order of expansion for the three components of $\boldsymbol{u}^k$ and σ_n. To meet well-known results from the literature (see, for example, Refs. 27 and 28 or the author's discussion reported in Refs. 7 and 8), different polynomial orders should be used in developments that are presented in the subsequent sections. Trace operators that would lead to a shortening of the resulting arrays in Eqs. (19) and (20) could be introduced for this aim. For the sake of brevity, the results related to these aspects have not been discussed. These could be more conveniently reported in future works.

V. Governing Equations

Equilibrium and compatibility are both formulated in terms of the $\boldsymbol{u}^k$ and σ^k_n unknowns via RMVT[5,6]:

$$\sum_{k=1}^{N_l} \int_{\Omega^k} \int_{A_k} \left[\delta \epsilon^{k^T}_{\mathrm{pG}} \sigma^k_{\mathrm{pH}} + \delta \epsilon^{k^T}_{\mathrm{nG}} \sigma^k_{\mathrm{nM}} + \delta \sigma^{k^T}_{\mathrm{nM}} (\epsilon^k_{\mathrm{nG}} - \epsilon^k_{\mathrm{nH}}) \right] \mathrm{d}\Omega^k \, \mathrm{d}z = \delta L^e \tag{14}$$

δ is the variational symbol. The left-hand side (LHS) includes the variations of the internal work in the plate: the first two terms come from classical displacement formulation, and they lead to variationally consistent equilibrium conditions; the third mixed term variationally enforces the compatibility of the transverse strain components.

A. Multilayer Case

Upon substitution of Eqs. (2), (3), and (12) and by integrating by parts, the RMVT leads to governing differential equations in terms of the introduced stress and displacement variables.

First, the multilayer modelings are considered. This leads to the equilibrium and constitutive governing equations in the each k-layer domain Ω^k. In compact form

$$\delta \boldsymbol{u}^k_\tau : \boldsymbol{K}^{k\tau s}_{uu} \boldsymbol{u}^k_s + \boldsymbol{K}^{k\tau s}_{u\sigma} \sigma^k_{\mathrm{ns}} = \boldsymbol{p}^k_\tau, \qquad \delta \sigma^k_{n\tau} : \boldsymbol{K}^{k\tau s}_{\sigma u} \boldsymbol{u}^k_s + \boldsymbol{K}^{k\tau s}_{\sigma\sigma} \sigma^k_{\mathrm{ns}} = 0 \tag{15}$$

with boundary conditions on Γ^k,

$$\boldsymbol{u}^k_\tau = \bar{\boldsymbol{u}}^k_\tau \quad \text{or} \quad \boldsymbol{\Pi}^{k\tau s}_u \boldsymbol{u}^k_s + \boldsymbol{\Pi}^{k\tau s}_\sigma \sigma^k_{\mathrm{ns}} = \boldsymbol{\Pi}^{k\tau s}_u \bar{\boldsymbol{u}}^k_s + \boldsymbol{\Pi}^{k\tau s}_\sigma \bar{\sigma}^k_{\mathrm{ns}} \tag{16}$$

The further subscript/superscript $s = t, b, r$ has been introduced in order to distinguish the terms related to the introduced variables from those related to their variations. The introduced differential operators are

$$\boldsymbol{K}^{k\tau s}_{uu} = -\boldsymbol{D}^T_p \boldsymbol{Z}^{k\tau s}_{\mathrm{pp}} \boldsymbol{D}_p, \qquad \boldsymbol{K}^{k\tau s}_{u\sigma} = -\boldsymbol{D}^T_p \boldsymbol{Z}^{k\tau s}_{\mathrm{pn}} + E_{\tau_z s} \boldsymbol{I} - E_{\tau s} \boldsymbol{D}^T_{n\Omega}$$

$$\boldsymbol{K}^{k\tau s}_{\sigma u} = E_{\tau s} \boldsymbol{D}_{n\Omega} + E_{\tau s_z} \boldsymbol{I} - \boldsymbol{Z}^{k\tau s}_{\mathrm{np}} \boldsymbol{D}_p, \qquad \boldsymbol{K}^{k\tau s}_{\sigma\sigma} = -\boldsymbol{Z}^{k\tau s}_{\mathrm{nn}}$$

$$\boldsymbol{\Pi}^{k\tau s}_u = \boldsymbol{I}^T_p \boldsymbol{Z}^{k\tau s}_{\mathrm{pp}} \boldsymbol{D}_p, \qquad \boldsymbol{\Pi}^{k\tau s}_\sigma = \boldsymbol{Z}^{k\tau s}_{\mathrm{pn}} + E_{\tau s} \boldsymbol{I}^T_{n\Omega} \tag{17}$$

where

$$\boldsymbol{I} = \begin{bmatrix} 1 & 0 & 0 \\ 0 & 1 & 0 \\ 0 & 0 & 1 \end{bmatrix}, \qquad \boldsymbol{I}_p = \begin{bmatrix} 1 & 0 & 0 \\ 0 & 1 & 0 \\ 1 & 1 & 0 \end{bmatrix}, \qquad \boldsymbol{I}_{n\Omega} = \begin{bmatrix} 0 & 0 & 1 \\ 0 & 0 & 1 \\ 0 & 0 & 0 \end{bmatrix}$$

The integration in the thickness coordinate has been a priori carried out as usual in two-dimensional modelings. The following layer-stiffnesses and integrals have been introduced:

$$(\boldsymbol{Z}^{k\tau s}_{\mathrm{pp}}, \boldsymbol{Z}^{k\tau s}_{\mathrm{pn}}, \boldsymbol{Z}^{k\tau s}_{\mathrm{np}}, \boldsymbol{Z}^{k\tau s}_{\mathrm{nn}}) = (\boldsymbol{C}^k_{\mathrm{pp}}, \boldsymbol{C}^k_{\mathrm{pn}}, \boldsymbol{C}^k_{\mathrm{np}}, \boldsymbol{C}^k_{\mathrm{nn}}) E_{\tau s}$$

$$(E^k_{\tau s}, E_{\tau_z s}, E_{\tau s_z}) = \int_{A_k} (F_\tau F_s, F_{\tau_z} F_s, F_\tau F_{s_z}) \, \mathrm{d}z \tag{18}$$

Further, subscript z denotes differentiation in the plate thickness coordinate. Explicit forms of the governing equations for each layer can be written by expanding the introduced subscripts and superscripts in the previous arrays, as follows:

$$k = 1, 2, \ldots, N_l; \qquad \tau = t, r, b, \qquad s = t, r, b, \qquad r = 2, \ldots N$$

The governing equations have been considered to be independent for each k layer. Interlaminar continuity at Eqs. (10), (11), and (13) can be enforced by writing the governing equations from a layer to a multilayered level. This procedure has been detailed in Refs. 7 and 9. At the very end the multilayer equations are formally written

$$\boldsymbol{K}_{uu}\boldsymbol{u} + \boldsymbol{K}_{u\sigma}\sigma_n = \boldsymbol{p} + \boldsymbol{p}_u^{1N_l}, \qquad \boldsymbol{K}_{\sigma u}\boldsymbol{u} + \boldsymbol{K}_{\sigma\sigma}\sigma_n = \boldsymbol{p}_\sigma^{1N_l} \tag{19}$$

with boundary conditions

$$\boldsymbol{u} = \bar{\boldsymbol{u}} \quad \text{or} \quad \boldsymbol{\Pi}_u\boldsymbol{u} + \boldsymbol{\Pi}_\sigma\sigma_n = \boldsymbol{\Pi}_u\bar{\boldsymbol{u}} + \boldsymbol{\Pi}_\sigma\bar{\sigma}_n \tag{20}$$

$\boldsymbol{p}_u^{1N_l}$ and $\boldsymbol{p}_\sigma^{1N_l}$ are the arrays obtained from the transverse stress values imposed at the top/bottom of the plate Eq. (11). The dimensions of the preceding multilayered arrays are given next: $\boldsymbol{u}, \boldsymbol{p}, \boldsymbol{p}_u^{1N_l}$ have $M_u = 3(N_l + 1) + 3(N - 1)N_l$ elements; whereas $\sigma, \boldsymbol{p}_\sigma^{1N_l}$ have $M_\sigma = M_u - 6$ elements; $\boldsymbol{K}_{uu}$ and $\boldsymbol{\Pi}_u$ have M_u-rows $\times$ M_u-columns; $\boldsymbol{K}_{u\sigma}$ and $\boldsymbol{\Pi}_\sigma$ have M_u-rows $\times$ M_σ-columns; $\boldsymbol{K}_{\sigma u}$ has M_σ-rows $\times$ M_u-columns; and $\boldsymbol{K}_{\sigma\sigma}$ has M_σ-rows $\times$ M_σ-columns.

B. Single-Layer Case

The unified notation introduced in Sec. III permits one the derivation of the governing equations related to single-layer modelings in a way exactly coincident to that used for multilayer case. The equilibrium and compatibility governing equations take the following form:

$$\delta\boldsymbol{u}_\tau\colon \boldsymbol{K}_{uu}^{k\tau s}\boldsymbol{u}_s + \boldsymbol{K}_{u\sigma}^{k\tau s}\sigma_{\text{ns}}^k = \boldsymbol{p}_\tau, \qquad \delta\sigma_{n\tau}^k\colon \boldsymbol{K}_{\sigma u}^{k\tau s}\boldsymbol{u}_s + \boldsymbol{K}_{\sigma\sigma}^{k\tau s}\sigma_{\text{ns}}^k = 0 \tag{21}$$

with boundary conditions

$$\boldsymbol{u}_\tau = \bar{\boldsymbol{u}}_\tau \quad \text{or} \quad \boldsymbol{\Pi}_u^{k\tau s}\boldsymbol{u}_s + \boldsymbol{\Pi}_\sigma^{k\tau s}\sigma_{\text{ns}}^k = \boldsymbol{\Pi}_u^{k\tau s}\bar{\boldsymbol{u}}_s + \boldsymbol{\Pi}_\sigma^{k\tau s}\sigma_{\text{ns}}^k \tag{22}$$

Displacement variables are not affected by the layer superscript k. Related arrays do not change dimensions when the equations are written at the multilayered level. In fact, these arrays simply accumulate layer-by-layer contributions when interface compatibility Eq. (13) is enforced. Interlaminar stress continuity can be imposed as for the multilayer case. Resulting multilayer equations take the same form of those depicted in Eqs. (19) and (20). The

Table 3 Effect of orthotropic ratio on transverse displacement and transverse shear-stress evaluations: comparison to three-dimensional analysis by Noor and Burton[31a]

		$U_z \times \left(E_T / P_{z_t}^{N_l} h\right)$				$S_{xz} \times \left(1 / P_{z_t}^{N_l}\right)$		
E_L / E_T		3	10	30		3	10	30
Exact	t	14.59	9.331	6.227	——	1.185	1.171	1.141
	b	14.17	8.929	5.838	——	——	——	——
LW-1	t	15.59	9.326	6.215	3D	1.183	1.170	1.139
	b	14.17	8.923	5.827	M	1.173	1.162	1.133
LW-2	t	15.59	9.221	6.277	3D	1.185	1.171	1.141
	b	14.17	8.929	5.838	M	1.185	1.170	1.138
LW-3	t	15.59	9.331	6.227	3D	1.185	1.171	1.141
	b	14.17	8.929	5.838	M	1.185	1.171	1.141
ESL-1	t	12.85	8.191	5.593	3D	1.195	1.194	1.189
	b	12.44	8.586	5.210	M	0.8202	0.8194	0.8172
ESL-2	t	14.58	8.992	5.704	3D	1.197	1.199	1.209
	b	14.16	8.590	5.316	M	0.8477	0.8241	0.8091
ESL-3	t	15.03	9.584	6.360	3D	1.180	1.167	1.136
	b	14.62	9.086	5.841	M	1.182	1.182	1.167

[a]Ten-layered plates with $a/h = 5$. Material data: $G_{TT}/E_T = 0.5$, $G_{TT}/E_T = 0.35$, $\nu_{TT} = 0.3$, and $\nu_{TT} = 0.49$.

Table 1 Maximum transverse displacement $U_z \times 100\ (E_T h^3 / P_{z_t}^{N_l} a^4)$ for a plate in cylindrical bending: comparison of present analyses to exact solutions and to other single-layer and multilayer analyses

	Case a: symmetrically laminated plates						Case b: asymmetrically laminated plates			
	$a/h = 4$			$a/h = 6$			$a/h = 4$		$a/h = 6$	
N_l	3	5	9	3	5	9	4	8	4	8
Exact[29]	2.887	3.044	3.324	1.635	1.721	1.929	4.181	3.724	2.556	2.224
				Multilayer theory LWM						
Ref. 2	2.907	3.059	——	——	——	——	4.202	——	——	——
LW-1	2.791	3.005	3.316	1.599	1.707	1.926	4.163	3.722	2.542	2.219
LW-2	2.891	3.048	3.324	1.635	1.721	1.929	4.181	3.730	2.556	2.231
LW-3	2.887	3.044	3.324	1.635	1.721	1.929	4.181	3.730	2.556	2.223
				Single-layer theory ESLM						
Ref. 1	2.907	3.018	3.231	1.636	1.702	1.875	3.316	3.225	2.107	1.934
Ref. 3	2.881	3.032	3.313	1.634	1.716	1.921	4.105	3.625	2.519	2.181
ESL-1	2.904	3.014	3.226	1.634	1.699	1.871	3.300	3.214	2.095	1.975
ESL-2	2.831	2.964	3.194	1.602	1.681	1.862	3.478	3.231	2.195	1.993
ESL-3	2.881	3.032	3.313	1.634	1.716	1.921	4.102	3.630	2.514	2.180

Table 2 Comparison to 3D analysis by Pagano and Hatfield[30] on transverse shear stresses $S_{xz} \times h/P_{z_t}^{N_l} a$ evaluated at $z = 0$ for three- and nine-layered plates

		$N_l = 3$					$N_l = 9$				
	a/h	2	4	10	20	100	2	4	10	20	100
Exact	——	0.153	0.219	0.301	0.328	0.339	0.204	0.223	0.247	0.255	0.259
LW-1	3D	0.164	0.229	0.304	0.329	0.339	0.196	0.223	0.247	0.255	0.259
	M	0.167	0.229	0.302	0.326	0.336	0.193	0.220	0.245	0.255	0.257
LW-2	3D	0.154	0.219	0.301	0.328	0.339	0.204	0.223	0.247	0.255	0.259
	M	0.155	0.221	0.302	0.328	0.339	0.204	0.223	0.247	0.255	0.259
LW-3	3D	0.154	0.219	0.301	0.328	0.339	0.204	0.223	0.247	0.255	0.259
	M	0.154	0.219	0.301	0.328	0.339	0.204	0.223	0.247	0.255	0.259
ESL-1	3D	0.155	0.219	0.300	0.327	0.338	0.220	0.222	0.244	0.254	0.258
	M	0.159	0.228	0.315	0.344	0.355	0.146	0.143	0.155	0.162	0.165
ESL-2	3D	0.153	0.219	0.302	0.328	0.338	0.221	0.221	0.244	0.254	0.259
	M	0.147	0.217	0.303	0.331	0.342	0.125	0.138	0.156	0.163	0.167
ESL-3	3D	0.149	0.217	0.301	0.328	0.339	0.190	0.221	0.246	0.255	0.259
	M	0.157	0.225	0.310	0.339	0.350	0.197	0.232	0.259	0.269	0.273

unique difference is related to the M_u dimension, which is now N_l-independent: $M_u = 3(N+2)$.

By employing the obtained constitutive equations, the stress variables can be eliminated in the numerical solution procedures. The problem is therefore reduced to displacement variables whose numbers are N_l-independent.

C. Closed-Form Solutions for Cross-Ply Laminated Plates

The boundary-values problem, governed by Eqs. (19) and (20) in the most general case of geometry, boundary conditions, and layouts, could be solved by implementing only approximated solution procedures. The particular case, in which the material has the properties $\tilde{C}_{16} = \tilde{C}_{26} = \tilde{C}_{36} = \tilde{C}_{45} = 0$, has here been considered, for which Navier-type closed-form solutions can be found by assuming the following harmonic forms for the applied loadings and unknown variables:

$$(u^k_{x_\tau}, \sigma^k_{xz_\tau}, p^k_{x_\tau}) = \sum_{m,n} (U^k_x, S^k_{xz_\tau}, P^k_{x_\tau}) \cos\frac{m\pi x}{a} \sin\frac{n\pi y}{b}$$

$$(u^k_{y_\tau}, \sigma^k_{yz_\tau}, p^k_{y_\tau}) = \sum_{m,n} (U^k_y, S^k_{yz_\tau}, P^k_{y_\tau}) \sin\frac{m\pi x}{a} \cos\frac{n\pi y}{b}$$

$$(u^k_{z_\tau}, \sigma^k_{zz_\tau}, p^k_{z_\tau}) = \sum_{m,n} (U^k_z, S^k_{zz_\tau}, P^k_{z_\tau}) \sin\frac{m\pi x}{a} \sin\frac{n\pi y}{b} \qquad (23)$$

where a and b are the plate lengths in the x and y directions, respectively, and m and n are the correspondent wave numbers. Capital letters on the right-hand side (RHS) are correspondent maximum amplitudes. On substitution of Eqs. (23), the governing equations assume the form of a linear system of algebraic equations. This procedure has been coded, and the results are discussed in the next section.

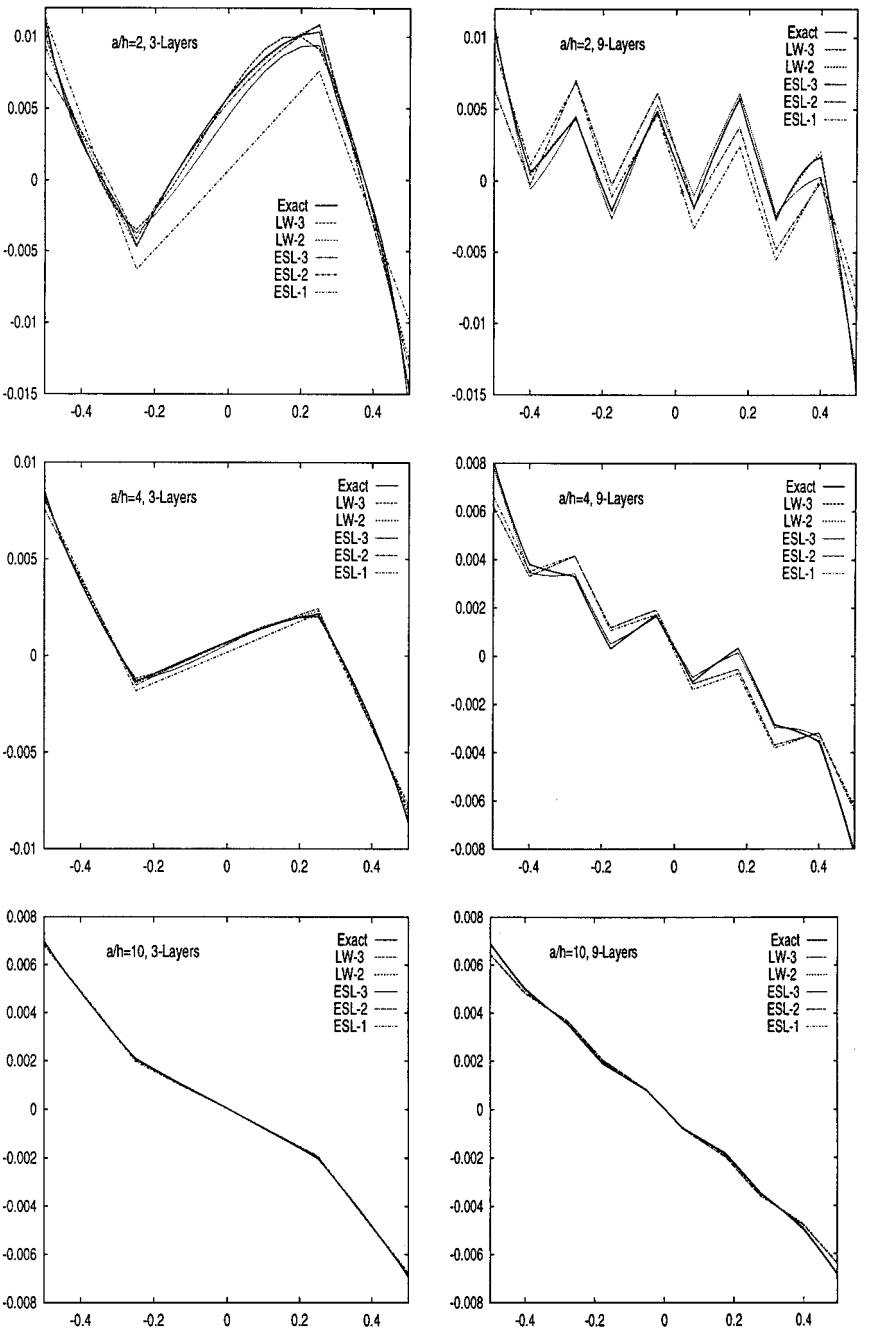

Case a: symmetrically laminated plates

Fig. 3 In-plane displacement $U_x \times (E_T h^2/P^{N_l}_{z_t} a^3)$ vs z. Influence of thickness ratio.

VI. Results and Discussion

Simply supported plates bend by a transverse bisinusoidal distribution of normal pressure applied to the top surface of the whole plate $p_{z_l}^{N_l}$ are considered. The two problems for which three-dimensional solutions are available have been discussed: cylindrical bending in the x direction ($m=1, n=0$) and square plates ($m=n=1$). Symmetrically, asymmetrically cross-ply laminated as well as thin, moderately thick, and very thick plates have been investigated. In-plane and out-of-plane stress and displacement results are discussed. Exception has been made for the Table 4 analysis in Ref. 29, where the following mechanical data of the lamina are used: $E_L = 25 \times 10^6$ psi, $E_T = 1 \times 10^6$ psi, $G_{LT} = 0.5 \times 10^6$ psi, $G_{TT} = 0.2 \times 10^6$ psi, $\nu_{LT} = \nu_{TT} = 0.25$; and where, following the usual notation,[24] L signifies the fiber direction, T the transverse direction and ν_{LT} is the major Poisson ratio. The material is assumed to be square-symmetric, and consistent units are referred to.

Four cases of multilayer theories have been considered in Eq. (12). Linear LW-1, parabolic LW-2, cubic LW-3, and fourth-order LW-4 expansion for $\boldsymbol{u}^k$ and σ_n^k. LW-1 and LW-2 were already considered in Ref. 9, whereas LW-3 and LW-4 have been implemented in this paper. The LW-1 case does not allow the fulfillment of the homogeneous transverse shear stress conditions on the bottom and top of the plates. This fact could lead to poorer results for plates with low N_l values.[9,10]

Three cases of single-layer expansions have been implemented and are denoted by the acronyms ESL-1, ESL-2, and ESL-3 in the subsequent tables and diagrams. These are, respectively, related to linear, parabolic, and cubic $\boldsymbol{u}$ fields and parabolic, cubic, and fourth-order σ_n^k fields. σ_{zz} were not included in the early ESL-1-type theory by Toledano and Murakami.[2] The ESL-2 case has been proposed in the present analysis. The ESL-3 model coincides with that presented in Ref. 3. Evaluations of transverse shear stresses were not quoted in Ref. 3.

Table 1 compares the transverse deflection of the midplane for thick plates under cylindrical bending. Cross-ply symmetrically and asymmetrically laminated plates (with equal thickness in each layer) have been considered. The results related to the present analysis are compared to the exact solutions by Pagano[29] and to other available

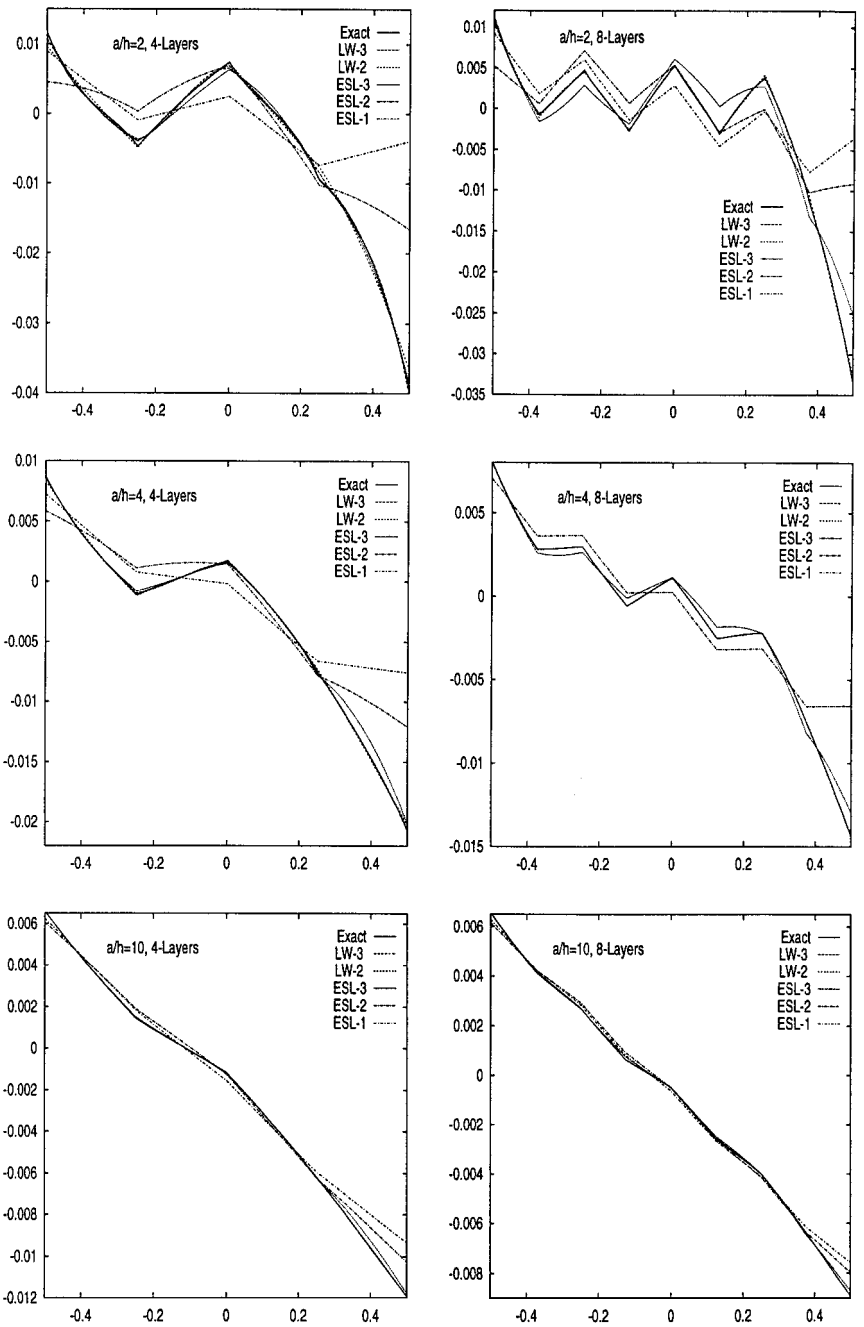

Case b: asymmetrically laminated plates

Fig. 3 In-plane displacement $U_x \times (E_T h^2/P_{z_l}^{N_l} a^3)$ vs z. Influence of thickness ratio (continued).

single-layer and multilayer results. Good accuracy has been found compared to the considered single-layer and multilayer results. The multilayer analysis matches the exact solution for both values of the considered thickness ratio with excellent accuracy. Such accuracy is confirmed for both symmetrically and asymmetrically laminated plates. Furthermore, the convergence rate related to the increasing order in the used expansion for $\boldsymbol{u}^k$ and σ_n^k increases with an increase in the number of the N_l layers. Quite different behavior has to be registered for the single-layer results. ESL-1 and ESL-2 work better for symmetrically laminated plates. ESL-2 and ESL-3 results show the effectiveness of parabolic terms in the $\boldsymbol{u}$ expansion for asymmetrically laminated plate analysis.

Transverse shear-stress evaluations are considered in Table 2. Two N_l values and very thick $(a/h = 2)$ and thin $(a/h = 100)$ plates have been investigated.[30] The stress values computed a priori in Eqs. (12) and a posteriori by integration of the three-dimensional indefinite equilibrium equations have been depicted by model (M) and a posteriori (3D), respectively. The conclusions drawn from an analysis of Table 1 can be extended to transverse shear stresses. It can be confirmed[9] that multilayer analyses lead to a priori evaluations of stress that are in excellent agreement with the exact solutions. The superiority of shear stresses evaluated 3D compared to those computed directly from the M must still be confirmed.[11,17]

These stresses are inaccurate even though thin plates have been investigated. The superiority of the multilayer analysis compared to single-layer ones is evident for very thick plate cases. The effect of the orthotropic ratio E_L/E_T has been investigated in Table 3 (Ref. 31) for both transverse displacement (top and bottom plate values are quoted) and transverse shear stress values (both 3D and M values are given). Most of the comments made for the preceding analysis can be extended to the Table 3 results. The accuracy of both LW and ESL analyses is not even slightly affected by E_L/E_T. This is a fundamental property of two-dimensional multilayered plate models that include zigzag effects and fulfill interlaminar equilibria.

A large investigation has been conducted to compare single-layer vs multilayer models for various geometrical parameter and

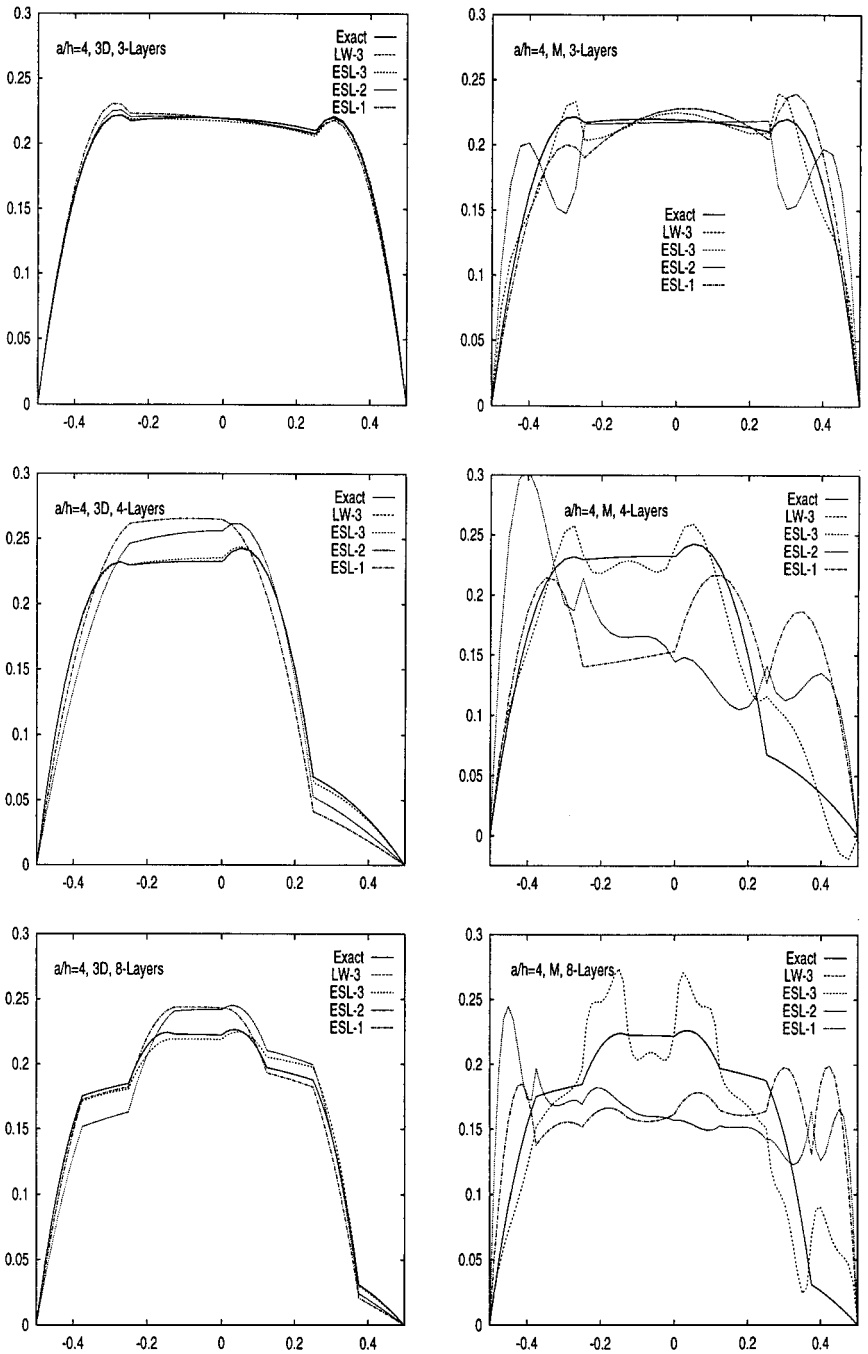

Case a: $a/h = 2$

Fig. 4 Transverse shear stress $S_{xz}(h/P_{zl}^{N_l}a)$ vs z. Comparison between values computed from the assumed model (M) and values obtained by integration of three-dimensional equilibrium equations (3D). Symmetrically and asymmetrically laminated plates.

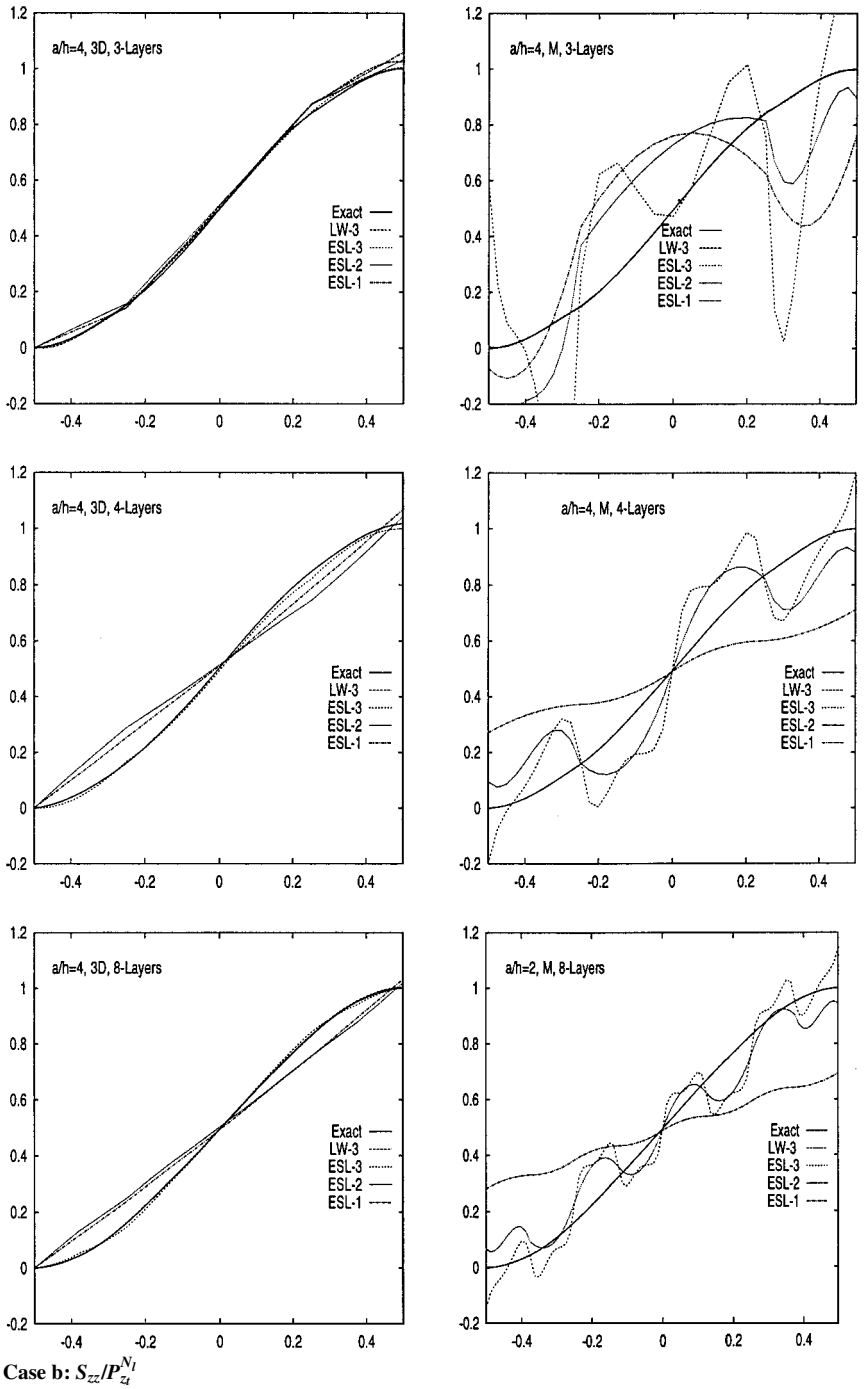

Fig. 4 Transverse shear stress $S_{xz}(h/P_{z_t}^{N_l}a)$ vs z. Comparison between values computed from the assumed model (M) and values obtained by integration of three-dimensional equilibrium equations (3D). Symmetrically and asymmetrically laminated plates (continued).

laminated layouts. Some of the most interesting, though not exhaustive, results are presented in Figs. 3–5, in the form of diagrams. All of the figures show the distribution of amplitudes of stress and displacements (as the ordinate) vs the plate thickness direction z/h (as the abscissa). The plate considered by Ref. 30 has been dealt with. Where not available, the exact solution has been considered to be coincident to the LW-4 results.

The influence of N_l on the in-plane displacement is analyzed in Fig. 3. Moderately thick ($a/h = 10$) and very thick ($a/h = 2$) plate geometries have been investigated. The LW-3 results coincide everywhere to the exact solution; the LW-2 results are very closed to the LW-3 analysis. The accuracy of the considered single-layer models is subordinate to the N_l and a/h values. ESL-1 and ESL-2 can be very inaccurate in predicting the in-plane response of thick, asymmetrically laminated plates with an increasing number of layers.

The a priori and a posteriori evaluation of transverse shear stress has been compared in Fig. 4. Symmetrically and asymmetrically laminated plates have been considered for both transverse shear and normal stresses. The thickness ratio is $a/h = 4$. The multilayer models match the exact solution very well. The single-layer results are less accurate than the displacement evaluations of Fig. 3. It can be confirmed that a priori evaluations of transverse stresses based on single-layer modelings can become ineffective. The thick, four-layered plate has shown negative values of transverse shear stress that correspond to the ESL-3 analysis. Furthermore, ESL models are not effective in furnishing a priori descriptions of σ_{zz}. The use of postprocessing, based on integration of a 3D indefinite equilibrium equation is mandatory in this case, whereas LW models do not require this postprocessing.

Very thick and thin nine-layered plates are considered in Fig. 5. M, 3D, and transverse shear stress directly obtained using Hooke's

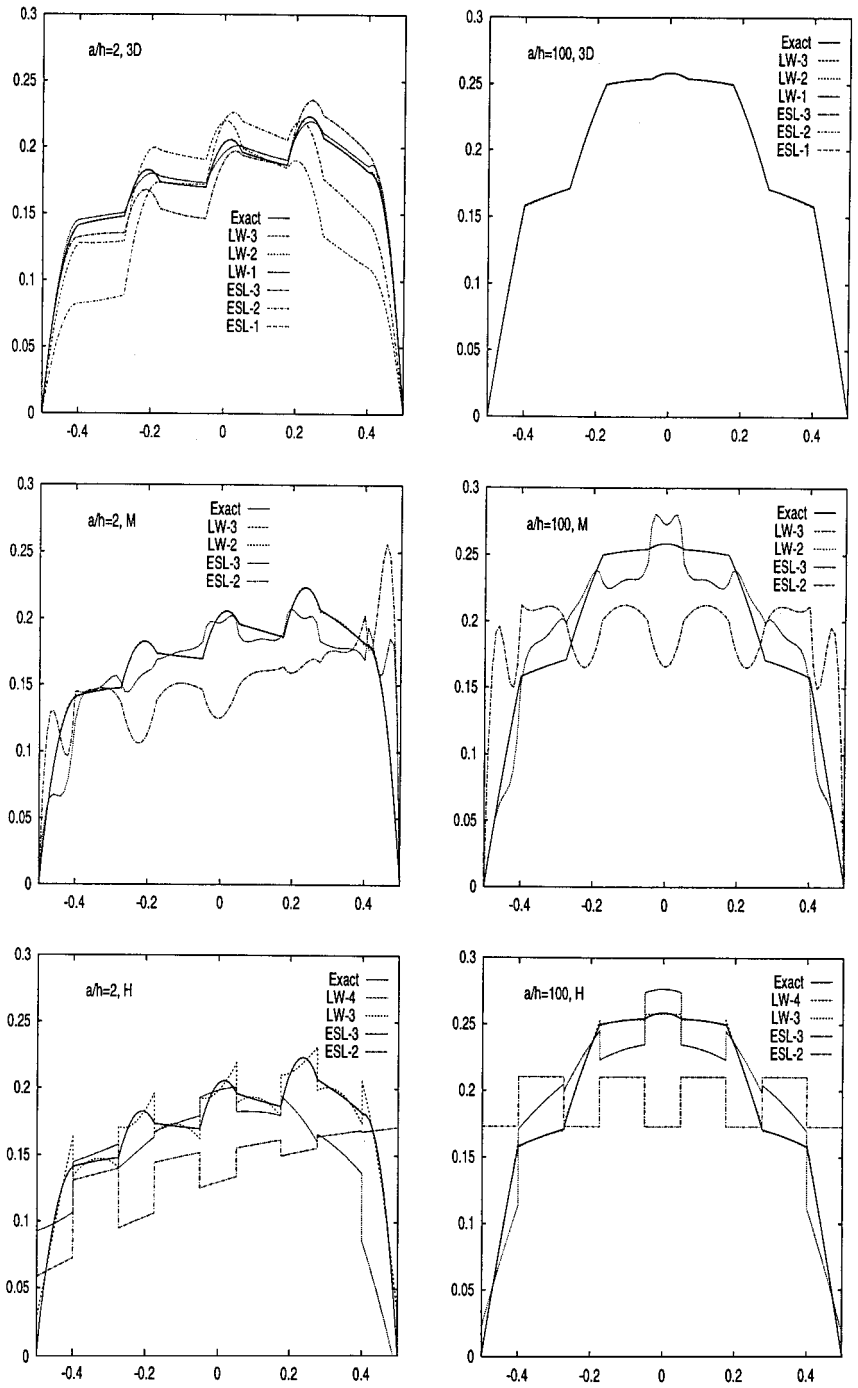

Fig. 5 Transverse shear stress $S_{xz}(h/P_{z_t}^{N_l}a)$ vs z. Comparison of values computed from the assumed model (M), values obtained by integration of 3D equilibrium equations (3D), and values calculated directly from Hooke's law (H). Symmetrically laminated nine layers thick and thin plates.

law (H) in Eqs. (2) are compared. What was found in the Table 2 analysis can be confirmed: single-layer models do not furnish accurate a priori evaluations of transverse stress fields even when thin plates are considered. H evaluations show that Hooke's law associated to higher expansion can be very effective in the framework of multilayer description. H evaluations are as inaccurate as the M results, as far as single-layer analyses are concerned.

VII. Conclusions

This paper has compared single-layer with multilayer theories formulated on the basis of RMVT. The zigzag form of the displacement fields as well as interlaminar equilibria for the transverse stresses (including normal component) are included in the formulations. A formalism has been introduced that has permitted the derivation of the governing equations in a unified manner. Results have been given for cross-ply laminated plates subjected to transverse harmonic loadings. From the conducted analysis the following main conclusions can be drawn:

1) It has been confirmed that the Reissner mixed variational is in fact a valuable tool to analyze multilayered plates.

2) Multilayer analyses furnish a quasi-three-dimensional description of displacement and stress fields even when very thick plates are considered ($a/h \leq 4$). Transverse stress evaluations do not require any postprocessing a posteriori procedure such as the integration of three-dimensional indefinite equilibrium equations. These stresses are in fact computed a priori and with excellent accuracy using the assumed models. Higher-order expansions have permitted accurate stress evaluations directly from Hooke's law.

3) The accuracy given by single-layer models is very much subordinate to the order of the used expansion in the displacement and stress fields, to laminate layouts and to geometrical parameters. The case of the cubic displacement field (ESL-3) has led to the best

results. Better evaluations have been found for transverse stresses calculated a posteriori than those furnished by the assumed model. Such a posteriori evaluations are required even though thin plates are considered.

It is the author's opinion that single-layer models could conveniently be employed to analyze the response of moderately thick ($a/h \geq 10$) and thick ($4 \leq a/h \leq 10$) plates. Single-layer models would be preferred in the framework of computational applications, i.e., finite element implementions. Nevertheless, a finite element formulation on the basis of multilayers theories, even though computationally expensive, could serve as a sample to assess simplified models (such as the single-layer analysis) for those problems in which exact or approximated three-dimensional solutions are not available or are difficult to obtain.

References

[1]Murakami, H., "Laminated Composite Plate Theory with Improved In-Plane Response," *Journal of Applied Mechanics*, Vol. 53, 1986, pp. 661–666.

[2]Toledano, A., and Murakami, H., "A Composite Plate Theory for Arbitrary Laminated Configurations," *Journal of Applied Mechanics*, Vol. 54, 1987, pp. 181–189.

[3]Toledano, A., and Murakami, H., "A Higher-Order Laminated Plate Theory with Improved In-Plane Responses," *International Journal of Solids and Structures*, Vol. 23, 1987, pp. 111–131.

[4]Toledano, A., and Murakami, H., "Shear Deformable Two-Layer Plate Theory with Interlayer Slip," *Journal of Engineering Mechanics*, Vol. 114, 1988, pp. 604–633.

[5]Reissner, E., "On a Certain Mixed Variational Theory and a Proposed Applications," *International Journal for Numerical Methods in Engineering*, Vol. 20, 1984, pp. 1366–1368.

[6]Reissner, E., "On a Mixed Variational Theorem and on a Shear Deformable Plate Theory," *International Journal of Numerical Methods in Engineering*, Vol. 23, 1986, pp. 193–198.

[7]Carrera, E., "A Class of Two Dimensional Theories for Multilayered Plates Analysis," *Atti Accademia delle Scienze di Torino, Mem Sci. Fis.*, Vols. 19–20, 1995, pp. 49–87.

[8]Carrera, E., "C_z^0-Requirements: Models for the Two-Dimensional Analysis of Multilayered Structures," *Composite Structures*, Vol. 37, No. 3/4, 1997, pp. 373–384.

[9]Carrera, E., "Evaluation of Layerwise Mixed Theories for Laminated Plates Analysis," *AIAA Journal*, Vol. 36, No. 5, 1998, pp. 830–839.

[10]Carrera, E., "Layer-Wise Mixed Models for Accurate Vibration Analysis of Multilayered Plates," *Journal of Applied Mechanics*, Vol. 65, Dec. 1998, pp. 820–828.

[11]Bhaskar, K., and Varadan, T. K., "Reissner's New Mixed Variational Principle Applied to Laminated Cylindrical Shells," *Journal of Pressure Vessel Technology*, Vol. 114, 1992, pp. 115–119.

[12]Jing, H.-S., and Tzeng, K.-G., "Refined Shear Deformation Theory of Laminated Shells," *AIAA Journal*, Vol. 31, No. 4, 1993, pp. 765–773.

[13]Carrera, E., "A Reissner's Mixed Variational Theorem Applied to Vibrational Analysis of Multilayered Shell," *Journal of Applied Mechanics*, Vol. 66, March 1999, pp. 69–78.

[14]Carrera, E.,"Multilayered Shell Theories Accounting for Layerwise Mixed Description, Part 1: Governing Equations," *AIAA Journal*, Vol. 37, No. 9, 1999, pp. 1107–1116.

[15]Carrera, E.,"Multilayered Shell Theories Accounting for Layerwise Mixed Description, Part 2: Numerical Evaluations," *AIAA Journal*, Vol. 37, No. 9, 1999, pp. 1117–1124.

[16]Rao, K. M., and Meyer-Piening, H. R., "Analysis of Thick Laminated Anisotropic Composites Plates by the Finite Element Method," *Composite Structures*, Vol. 15, 1990, pp. 185–213.

[17]Carrera, E., "C^0 Reissner-Mindlin Multilayered Plate Elements Including Zig-Zag and Interlaminar Stresses Continuity," *International Journal for Numerical Methods in Engineering*, Vol. 39, 1996, pp. 1797–1820.

[18]Carrera, E., and Kröplin, B., "Zig-Zag and Interlaminar Equilibria Effects in Large Deflection and Postbuckling Analysis of Multilayered Plates," *Mechanics of Composite Materials and Structures*, Vol. 4, 1997, pp. 69–94.

[19]Carrera, E., "An Improved Reissner-Mindlin-Type Model for the Electro-Mechanical Analysis of Multilayered Plates Including Piezo-Layers," *Journal of Intelligent Materials System and Structures*, Vol. 8, 1997, pp. 232–248.

[20]Carrera, E., and Krause, H., "An Investigation on Nonlinear Dynamics of Multilayered Plates Accounting for C_z^0 Requirements," *Computers and Structures*, Vol. 69, 1998, pp. 463–486.

[21]Carrera, E., "A Refined Multilayered Finite Element Model Applied to Linear and Nonlinear Analysis of Sandwich Structures," *Composite Science and Technology*, Vol. 58, 1998, pp. 1553–1564.

[22]Bhaskar, K., and Varadan, T. K., "A Higher-Order Theory for Bending Analysis of Laminated Shells of Revolution," *Computer and Structures*, Vol. 40, 1991, pp. 815–819.

[23]Carrera, E., and Parisch, H., "Evaluation of Geometrical Nonlinear Effects of Thin and Moderately Thick Multi-Layered Composite Shells," *Composite Structures*, Vol. 40, 1998, pp. 11–23.

[24]Reddy, J. N., *Mechanics of Laminated Composite Plates, Theory and Analysis*, CRC Press, Boca Raton, FL, 1997.

[25]Cho, M., and Parmerter, R. R., "Efficient Higher Order Composite Plate Theory for General Lamination Configurations," *AIAA Journal*, Vol. 31, 1993, pp. 1299–1305.

[26]Lee, D., Waas, A. M., and Karnopp, B. H., "Analysis of Rating Multi-Layer Annular Plate Modeled via Layerwise Mixed Theory: Free Vibration and Transient Analysis," *Computers and Structures*, Vol. 66, 1998, pp. 313–335.

[27]Reissner, E., "Reflections on the Theory of Elastic Plates," *Applied Mechanics Review*, Vol. 38, 1985, pp. 1433–1464.

[28]Sun, C. T., and Whitney, J. M., "On the Theories for the Dynamic Response of Laminated Plates," *AIAA Journal*, Vol. 11, 1973, pp. 372–398.

[29]Pagano, N. J., "Exact Solutions for Composite Laminates in Cylindrical Bending," *Journal of Composite Material*, Vol. 3, 1969, pp. 398–411.

[30]Pagano, N. J., and Hatfield, S. J., "Elastic Behavior of Multilayered Bidirectional Composites," *AIAA Journal*, Vol. 10, 1972, pp. 931–933.

[31]Noor, A. K., and Burton, W. S., "Stress and Free Vibration Analyses of Multilayered Composite Plates," *Composite Structures*, Vol. 11, 1989, pp. 183–204.

A. M. Waas
Associate Editor